Charge disproportionation and dynamics in θ-(BEDT-TTF)$_2$CsZn(SCN)$_4$

R. Chiba,* K. Hiraki, and T. Takahashi
Department of Physics, Gakushuin University, Mejiro, Tokyo 171-8588, Japan

H. M. Yamamoto
The Institute of Physical and Chemical Research, 2-1 Hirosawa, Wakou 351-0198, Japan

T. Nakamura
Institute for Molecular Science, Myodaiji, Okazaki 444-8585, Japan

(Received 20 September 2007; revised manuscript received 7 January 2008; published 10 March 2008)

The electronic state of two-dimensional organic conductor, θ-(BEDT-TTF)$_2$CsZn(SCN)$_4$, has been investigated by means of ^{13}C-NMR line shape analyses on selectively ^{13}C-enriched single crystal sample. Strong charge disproportionation was found to develop in the "metallic" state well above metal-insulator transition temperature of ~20 K. The charge disproportionation becomes almost static below ~140 K, forming a short-range charge ordering, but no long-range ordering is stabilized at low temperatures down to 5 K. About half of the molecular sites become nonmagnetic, while the other half carries finite magnetic moments. Charge disproportionation becomes very much reduced at least at the nonmagnetic molecular sites, implying that charge rearrangement occurs at ~20 K.

DOI: 10.1103/PhysRevB.77.115113 PACS number(s): 71.20.Rv, 71.30.+h, 76.60.−k

I. INTRODUCTION

Charge ordering (CO) phenomena are attracting wide interest in research in the field of organic molecular conductors.[1–3] It has been well established that the CO state is one of typical ground states of the so-called 2:1 type charge transfer molecular complexes with quasi-one-dimensional[4–10] and two-dimensional (2D) conductions.[11–14] It is a novel manifestation of the Coulomb correlation, where not only the short-range (on-site) Coulomb repulsion U[15] but also intersite components V_{ij} are responsible.[16] Increasing numbers of material have been experimentally revealed to exhibit various types of CO ground states,[1] and many theoretical trials have been proposed to describe the diverse electronic states based on different molecular arrangements in a systematic way.[2,3]

In addition to the long-range (LR) CO ground states, novel features closely related to the charge degree of freedom have been found in the vicinity of long-range CO states. Competition between different types of COs can be tuned by applying pressure, leading to charge disproportionation (CD) without LR-CO, a charge-glass state and/or a melting of CO. In a typical one-dimensional CO system, (DCl-DCNQI)$_2$Ag,[4] Itou *et al.* reported that the CO ground state melts under pressure into a three-dimensional liquid with cubic temperature dependence of resistivity,[17] which implies an unprecedented mechanism of electron-electron scattering. In a 2D CO system, θ-(BEDT-TTF)$_2$RbZn(SCN)$_4$, large CDs with extremely slow fluctuations have been found to develop already in the metallic region above the transition temperature.[18] A similar but different type of CD was found in another 2D-CO system, α-(BEDT-TTF)$_2$I$_3$, at temperatures well above the transition temperature.[13,14,19] Short-range charge orders were found to coexist with metallic behavior in some organic materials,[20] as well as in inorganic oxides.[21]

θ-ET$_2$RbZn(SCN)$_4$ (abbreviated as RbZn salt, hereafter) is a well-known 2D-CO system. The CO below the metal-insulator transition at 190 K was confirmed by NMR,[11,12] x ray,[22] vibrational spectroscopy,[23] and optical conductivity.[24] There had been synthesized a series of θ-phase compounds, which have a characteristic donor arrangement with high symmetry in the conducting 2D layers. Mori *et al.* found a systematic relation between the molecular arrangement (actually, the dihedral angle between adjacent donor molecules in the conducting layer) and the metal-insulator transition temperature; the larger dihedral angle gives the higher metal-insulator transition temperature.[25] A sister member of the RbZn salt, θ-ET$_2$RbCo(SCN)$_4$, was confirmed to have a CO state.[26] Recently, the CO in θ-ET$_2$TlZn(SCN)$_4$ was also observed.[27]

The title compound, θ-ET$_2$CsZn(SCN)$_4$ (abbreviated as CsZn salt, hereafter), is a member of the θ-phase compounds, which has a crystal structure almost identical with that of the RbZn salt with a slightly smaller dihedral angle (105°) than that of the latter (111°). It behaves metallically at high temperatures with a broad resistance minimum around 100 K and a rapid increase of resistance is observed only below 20 K.[25,28] Magnetic susceptibility decreases monotonously with decreasing temperature down to 20 K, below which a Curie-like behavior appears.[25] However, electron paramagnetic resonance (EPR) measurements by Nakamura *et al.* suggested a spin-singlet ground state below 20 K.[29] Contrary to the case of the RbZn salt, no long-range order was observed by x-ray measurements down to low temperatures, while short-range lattice modulations with different wave numbers develop below ~120 K.[30,31] Mori *et al.* pointed out that the metal-insulator transition around 20 K of the CsZn salt should be qualitatively different from that of the RbZn salt by considering the transition behaviors in alloyed compounds, θ-ET$_2$Rb$_x$Cs$_{1-x}$Zn(SCN)$_4$.[32]

Recently, Terasaki and co-workers have discovered a giant nonlinear resistance effect in θ-ET$_2$CsM'(SCN)$_4$

$[M'=\mathrm{Co,Zn}]$ and attributed it to the competition between the different short-range orders.[33,34] Moreover, they observed the "melting" of insulating domains by applying large electric current.[34] It is believed that short-range CO's suggested by lattice modulations are responsible for these interesting anomalous behaviors. The CsZn salt is another interesting system where short-range CO's play essential roles in the vicinity of long-range CO state.

The purpose of the present work is to clarify the existence of possible short-range CO's in the CsZn salt and to investigate their dynamical properties by means of ^{13}C-NMR line shape analyses on selectively ^{13}C-enriched single crystal sample. We also measured spin-spin relaxation rate or homogeneous linewidth, $1/T_2$, which is a powerful probe of slow dynamics of the local fields seen by the probe nuclei with a characteristic frequency of the order of the linewidth approximately-several kilohertz.[18,35] While some of the experimental results have already been mentioned in several previous papers,[36–38] we will describe here the details of the measurements, the procedure of the analyses, and the pictures of the electronic state derived from the observations mentioned

The paper is organized as follows. Experimental details are described in Sec. II. In Sec. III, experimental results and discussions are given. After taking an overview of temperature dependence of ^{13}C-NMR spectrum, precise angular dependences of the spectrum in the *ab* plane at three typical temperatures, room temperature (295), 110, and 5 K, are shown and discussed in Secs. III A–III C, respectively. Homogeneous spectra obtained by fast Fourier transformation (FFT) of echo-decay curve are compared with inhomogeneous ones and the dynamics of charge fluctuation are analyzed in Sec. III D. Inhomogeneous spectra are analyzed in order to investigate the features of CD in Sec. III E. In Sec. III F, results of ^{13}C-NMR are compared with related experiments and theories. Conclusions are given in Sec. IV.

II. EXPERIMENT

Single crystals of the title compound were prepared on the basis of BEDT-TTF molecule in which the central double-bonded carbon sites were selectively replaced with ^{13}C isotope ($I=1/2$). ^{13}C-NMR measurements were performed on single crystal samples of a few milligrams in weight. Resonance frequency was 88 MHz, which corresponds to a resonance field of 8.2 T.

Absorption spectra were usually obtained by the FFT of spin echo signals following $\pi/2$-π pulse sequences. We also used free induction decay (FID) signals after $\pi/2$ pulse to get spectrum through FFT. Spectral shifts, such as center of mass of spectrum and peak positions, were measured with respect to the resonance position of ^{13}C nuclei in tetramethylsilane (abbreviated as TMS) as reference. Angular dependence of the spectrum was measured using a home-made NMR probe with a rotating sample holder.

III. RESULTS AND DISCUSSIONS

Figure 1 shows the temperature dependence of ^{13}C-NMR spectrum when the external field was applied perpendicular to the conducting plane (parallel to *a* axis; $\phi\sim 90°$). At room temperature, the spectrum consists of several (actually four) sharp peaks. This is well explained as a quartet structure which is characteristic of dipolar-coupled ^{13}C nuclei. Below 180 K, the spectrum becomes significantly broadened. At low temperatures, the spectrum becomes two broad peaks mainly due to nuclear dipolar coupling with excess asymmetric tail.

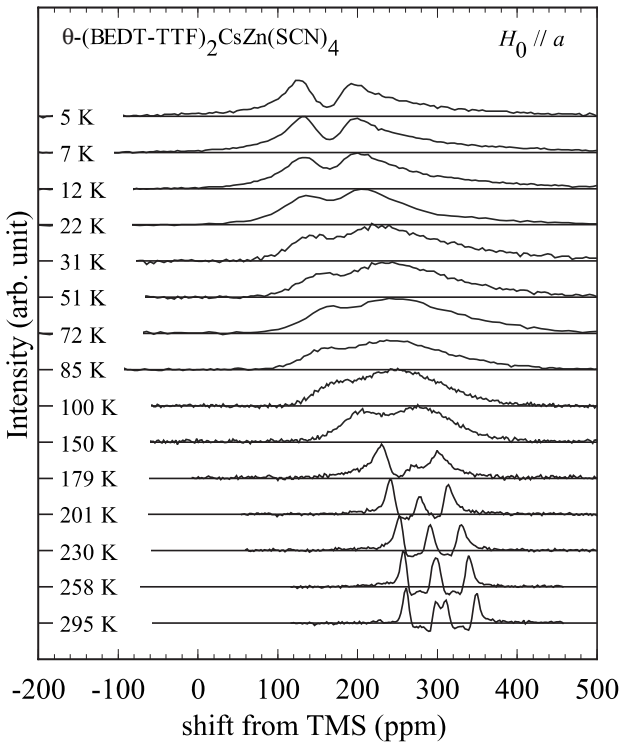

FIG. 1. Temperature dependence of ^{13}C-NMR spectrum when the external field is applied along the *a* axis.

Temperature dependences of the central shift and the second moment of the observed spectrum are plotted in Fig. 2 closed circles and closed squares, respectively). Center of mass of the spectrum exhibits a small temperature dependence, which seems to be well scaled to that of static susceptibility.[29] Below 30 K, the central shift starts to decrease suggesting a partial reduction of static susceptibility, while the reported susceptibility data exhibited a Curie tail corresponding to paramagnetic impurities.[29] Drop of central shift can be observed more clearly when the external field was applied along the *c* axis, since the Knight shift is much larger in this direction.[39] Details are published separately.

The second moment at high temperatures comes from the peak structure, whose contribution is estimated as 3.7 kHz^2. Excess broadening appears below $\sim$180 K. It should be noted that there appears no sharp structure as observed in the RbZn salt at low temperatures. This indicates that there is no long-range charge ordering even below the metal-insulator transition around 20 K.

In order to analyze the nature of the electronic state in each of the different temperature regions, precise angular dependence of the ^{13}C-NMR spectrum was measured at

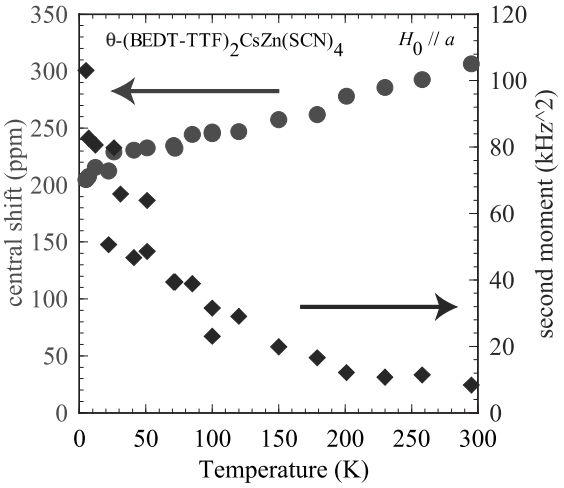

FIG. 2. Temperature dependence of the central shift $\bar{K}$ and the second moment of ^{13}C-NMR spectrum shown in Fig. 1.

room temperature (295), 101, and 5 K. The external field was rotated in the *ab* plane, where all BEDT-TTF molecules are crystallographically equivalent with respect to the field.

A. Angular dependence at room temperature

Angular dependence of ^{13}C-NMR spectrum at room temperature is shown in Fig. 3(a). All spectra were obtained by FFT of FID signals. At each direction of the field, the spectrum is composed of at most four sharp peaks, which is just expected for coupled ^{13}C pairs with a finite shift asymmetry.[40–42] Peak positions K and intensity I for coupled nuclei are given as follows:

$$K_{\mathrm{a}} = \bar{K} - \frac{1}{3}d - \frac{1}{2}\sqrt{\left(\frac{1}{3}d\right)^2 + \Delta K^2}, \quad I_{\mathrm{a}} = 1 + \sin 2\Theta,$$

$$K_{\mathrm{b}} = \bar{K} - \frac{1}{3}d + \frac{1}{2}\sqrt{\left(\frac{1}{3}d\right)^2 + \Delta K^2}, \quad I_{\mathrm{a}} = 1 - \sin 2\Theta,$$

$$K_{\mathrm{c}} = \bar{K} + \frac{1}{3}d - \frac{1}{2}\sqrt{\left(\frac{1}{3}d\right)^2 + \Delta K^2}, \quad I_{\mathrm{a}} = 1 - \sin 2\Theta,$$

$$K_{\mathrm{d}} = \bar{K} + \frac{1}{3}d + \frac{1}{2}\sqrt{\left(\frac{1}{3}d\right)^2 + \Delta K^2}, \quad I_{\mathrm{a}} = 1 + \sin 2\Theta,$$

where $\bar{K}$, ΔK, and d are central shift, shift asymmetry, and the splitting due to the dipolar coupling between ^{13}C nuclei, respectively. The relative intensity I depends on these parameters through $\sin 2\Theta = 1 - (d/3)/\sqrt{(d/3)^2 + \Delta K^2}$. We could experimentally determine these three parameters for each spectrum; the angular dependences of these parameters are plotted in Fig. 4. The parameter d is the separation of the Pake doublet and determined as $d = (3\gamma^2\hbar/2r^3)|1 - 3\cos^2\phi|$, with the gyromagnetic ratio, γ of ^{13}C nucleus, the Planck constant $\hbar$, the distance between two ^{13}C nuclei, $r \sim 1.4$ Å,[43] the angle ϕ between the external field H_0, and the ^{13}C=^{13}C vector ($\phi = 0°$ for $H_0 \| a$ and 90° for $H_0 \| b$). Note that the angular dependence of dipolar splitting d agrees well with expected one (the solid curve).

The shift asymmetry ΔK in the CsZn salt is about half as large as that in the RbZn salt.[18] ΔK should reflect the asymmetry of the surroundings of ET molecule. We thus think that this comes from the difference in crystal structure. These results imply that all ET molecular sites are electronically equivalent at room temperature; the effective charge of ET molecule should be considered to be one-half, $ET^{+0.5}$, as far as NMR properties are concerned.

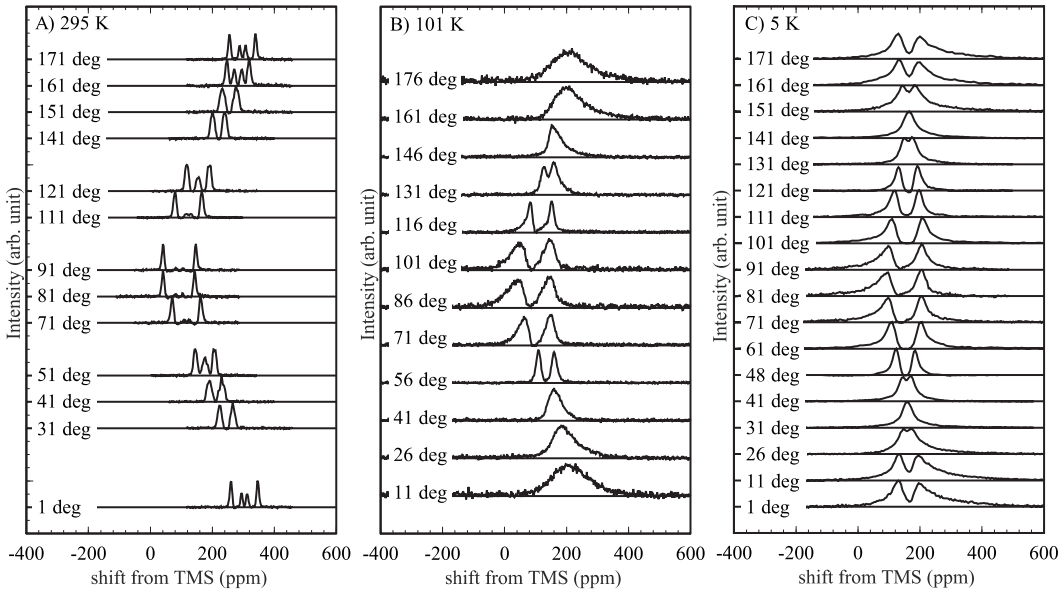

FIG. 3. Angular dependence of NMR line shape at room temperature, 101, and 5 K, respectively, where the external field is applied in the *ab* plane.

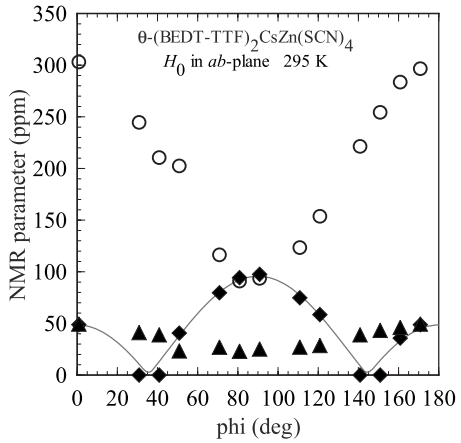

FIG. 4. Angular dependence of three parameters characterizing the observed ^{13}C-NMR spectrum at 298 K central shift $\bar{K}$ (open circles), shift asymmetry ΔK (closed triangles), and nuclear dipolar splitting d (closed diamonds).

B. Angular dependence of linewidth at 100 K: Charge disproportionation

The remarkable broadening observed below 180 K should be due to charge disproportionation, as observed in the RbZn salt just above the transition temperature T_{MI}. To confirm this speculation, we measured the angular dependence of the spectrum in the *ab* plane at 101 K. Results are shown in Fig. 3(b). We found that the excess broadening was remarkably angular dependent: it is the largest for $H_0 \| a$ (ϕ=0°), passing through the minimum and then becomes larger again around $H_0 \| b$ (ϕ=90°). The minimum appears at angles where the central shift crosses over ~150 ppm. Since the chemical shift for (BEDT-TTF)$^{0.5+}$ is estimated as 150 ppm and almost independent of angle in the CsZn salt, these angles correspond to those at which the Knight shift vanishes. Figure 5 shows the angular dependence of the excess broadening (the second moment subtracted nuclear dipolar contribution), $\langle \Delta f^2 \rangle_{\mathrm{excess}} = \langle \Delta f^2 \rangle_{\mathrm{obs}} - \langle \Delta f^2 \rangle_{\mathrm{dip}}$, in comparison to the square of the Knight shift K^2; these quantities are proportional to each other very well. This clearly means that the broadening is due to the inhomogeneity of the Knight shift, that is, the local fields at ^{13}C sites are inhomogeneously distributed. Thus, the remarkable line broadening below 180 K is a direct evidence of the appearance of strong charge disproportionation.

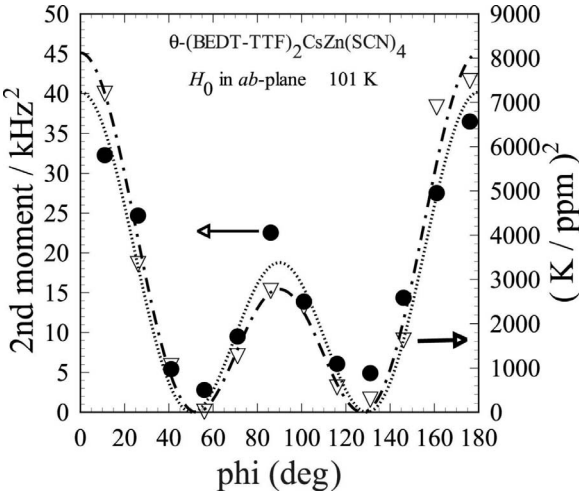

FIG. 5. Angular dependence of the second moment (closed circles) of the ^{13}C-NMR spectrum at 101 K, in comparison to the square of the Knight shift at the center of mass $\bar{K}$ (open triangles).

The situation is quite similar to the case of the RbZn salt above the transition. In the RbZn salt, a rather large offset of the second moment (~10 kHz^2) was observed at the minimum position. This value was reasonably explained as the contribution of ΔK, which remains finite at the zero Knight shift position. In the CsZn salt, the offset of the second moment is much smaller than that in the RbZn salt, as seen in Fig. 5. ΔK in this direction is ~3.1 kHz. From this value, the second moment at this angle is estimated as $\sim(3.1/2)^2$ ~2.4 kHz^2, which is consistent with the observed offset of ~3.8 kHz^2.

From the plots in Fig. 5, we obtain $\langle \Delta f^2 \rangle_{\mathrm{excess}} / K^2 \sim 0.63$. If we assume a linear relation between charge distribution and the line broadening, the standard deviation around the mean value of +0.50 is evaluated as $0.5 \times \sqrt{0.63} \sim 0.40$. This value is too large; a homogeneous distribution within the range between 0 and 1 gives a standard deviation of $1/2\sqrt{3}$ ~0.29. The value of 0.4 corresponds to a discrete distribution peaking at 0.1 and 0.9.

It should be noted that the spectrum at 100 K looks quite asymmetric. We believe that this asymmetry is intrinsic. Generally, care must be taken, since the spin echo signals following $\pi/2$-π pulse sequences may lead to an artifactual line shape, when dipolar broadening is dominant. In the present system, however, the broadening is found to be inhomogeneous and the homogeneous dipolar contribution is much smaller than the observed width, as shown in Sec. III D. Our pulse sequence is appropriate in this situation. It seems natural to try to decompose the spectrum into one or two peaks and an asymmetric tail leaning to one side. The tail component has the same anisotropy of the central shift as that of the Knight shift at room temperature. The center of mass of the whole spectrum is affected by this tail component.

In the RbZn salt, the broadening of the spectrum above the transition was almost symmetric, while a decomposition into sharp peaks and a broad component appeared below T_{MI}.[11,12] The former peaks were attributed to those from charge-poor sites and the latter from charge-rich sites. The width of the broad component was too large to detect precisely and never analyzed quantitatively. One can expect that the localized charges on the charge-rich sites produce another mechanism of line broadening, such as dipolar fields from neighboring molecular sites.

Comparing with this situation in the RbZn salt, the asymmetry may indicate a possible decomposition into charge-rich and charge-poor sites. Such decomposition, if any, should not be perfect, however, since the peaks are much broader and the tail is much shorter than those observed in the RbZn salt below T_{MI}.[11,12] No long-range charge order was observed at all measured temperatures in the CsZn salt,

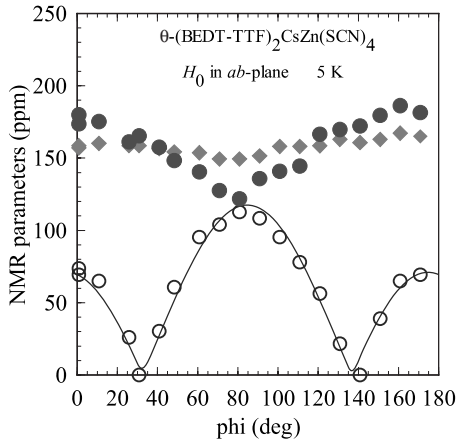

FIG. 6. Angular dependence of central shift (closed circles) and peak separation (open circles) of the observed ^{13}C-NMR spectrum at 5 K. Closed diamonds indicate the central position of the peak component.

but some short-range orderings may start to develop in this temperature range.

This consideration forces us to give up the hope of estimating the degree of charge distribution from the inhomogeneous width at least at this temperature (100 K) for the broad component. We will be back to this issue later in the analysis of temperature dependence of the spectrum at magic angle condition.

C. Angular dependence at 5 K: Nature of the insulating state below 20 K

The angular dependence of ^{13}C-NMR spectrum at 5 K is shown in Fig. 3(c). The spectrum consists of two broad peaks and an asymmetric tail. Central shift and peak separation of the observed spectrum are shown in Fig. 6. We plotted two measures of central position: the center of the peaks (closed diamonds) and the center of mass (the first moment, closed circles) of the whole spectrum. The center of the peaks are almost constant in this field rotation, while the center of mass shows a small anisotropy similar to those of the Knight shift observed at higher temperatures.

In the charge-ordered state of the RbZn salt at the same temperature, we observed four ^{13}C-NMR peaks (two sets of the Pake doublet) showing a remarkable angular dependence in the same geometry as in the present experiment.

Comparing with the angular dependence of the chemical shift in neutral BEDT-TTF molecules, two doublets were assigned to the charge-rich and charge-poor molecular sites, respectively, without any Knight shift; all spins are coupled to form spin singlets of the spin Peierls type. Note that the chemical shift strongly depends on the charge of the ET molecule. However, the angular dependences of the chemical shift for both sites are cancelled out with each other, so that the center of mass of the whole spectrum has no angular dependence; there must be a physical reason for this behavior, but we cannot figure it out at the moment.

The spectrum in the CsZn salt is in contrast to the one in the RbZn salts. It consists of two broad peaks and an asymmetric tail, instead of four sharp peaks. The center of the peaks has little angular dependence, resembling neither that for the charge-rich nor for the charge-poor sites.

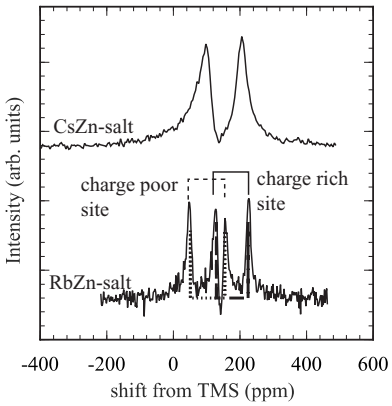

FIG. 7. Comparison of NMR line shapes of the CsZn salt and the RbZn salts at 5 K. External field was applied parallel to the *a* axis.

One of the simple explanations of the spectrum is to attribute the peaks and the tail components to the charge-poor and the charge-rich sites, respectively, as considered for the results at 101 K. However, this picture has a difficulty that the angular dependence of the center of peaks cannot be explained; the chemical shift for the charge-poor sites in the RbZn salt has the same asymmetry as that of the Knight shift in this field rotation, so that there is no reason for the disappearance of the angular dependence.

The only possible explanation is that the molecular sites responsible for the peak component have (i) an averaged charge of +0.5 and (ii) vanished local spin susceptibility, while the tail component comes from the site with a finite spin susceptibility. This picture is quite different from the previous one for the results at 101 K.

In order to accept this, there must be some transition or crossover in the electronic states somewhere between 100 and 5 K. We will discuss this issue later in comparison to other experimental results.

We note that the peaks are much broader than those observed in the RbZn salt. The excess broadening must be caused by charge disproportionation around the average value of ~0.5 through the inhomogeneity of the chemical shift, but not of the spin susceptibility, since the latter is almost lost for the peak components. We try to estimate the degree of the disproportionation using the spectrum at $\phi \sim 90°$ (the external field is parallel to the *a* axis), which is shown in Fig. 7 in comparison to that of the RbZn salt. The full widths at half maximum of the peak components are ~51.8 and 41.0 ppm for the lower and higher frequency peaks, respectively; the corresponding second moments assuming a Gaussian line shape are ~484 and ~303 ppm^2, while the homogeneous second moment measured at 5 K is ~8.7 ppm^2. Thus, the inhomogeneous broadenings of each peak are estimated as $\sim \pm 21.8$ and ± 17.2 ppm. The differences in the chemical shift between the charge-rich (+0.8) and the charge-poor (+0.2) sites in the RbZn salt were the largest in this direction, 78.0 ppm and 69.4 ppm for the lower and higher frequency peaks; the distribution of effec-

tive charge on the corresponding ET molecule should be $\sim 0.50 \pm 0.16$ (standard deviation assuming the Gaussian distribution). This is much smaller than the value estimated at higher temperatures (see also Sec. III E).

The separation of the peaks mainly comes from the nuclear dipolar coupling between the double-bonded central carbons, since the angular dependence of the separation is quite similar to the one expected for this coupling, as shown in Fig. 6. It should be noted, however, that the observed separation is systematically larger (about 20%) than the calculated one. It is a strong contrast to the case in the nonmagnetic charge-ordered state in the RbZn salt, where there was no deviation in the observed values from the calculated ones. The deviation is well explained if one assumes a finite asymmetry of the shift, $\Delta K \sim 40$ ppm. This may suggest that there remains some asymmetry in the resonance shift even the anisotropic component has almost vanished.

Contrary to the center of peaks, the first moment of the whole spectrum shows an anisotropy similar to those of the Knight shift observed at higher temperatures, as shown in Fig. 6. The first moment clearly contains the large contribution of the long and asymmetric tail component and may have some quantitative ambiguity. The amplitude of the angular dependence of the central shift is ~50 ppm at 5 K, which is about one-forth of the value of ~210 ppm at room temperature. Taking the center of the peaks ~160 ppm as the zero Knight shift position, the isotropic shifts of the whole spectrum are $300-160 \sim 140$ ppm and $200-160 \sim 40$ ppm at room temperature and at 5 K, respectively. The isotropic and anisotropic components of the Knight shift are well scaled with each other.

The estimation of the relative intensity of the tail component is difficult, but it is about one-half of the integrated total intensity. This fact seems to rule out the possibility that the tail component may be attributed to the impurity sites detected by susceptibility measurement. Roughly speaking, the half of the ET molecules lose their local spin susceptibility at low temperatures, but the other half does not.

D. Homogeneous and inhomogeneous spectra at magic angle

In order to analyze the dynamics of charge disproportionation, we have measured homogeneous line shape and compare it with inhomogeneous line shape, just as in the previous report on the RbZn salt.[18] Inhomogeneous line shapes were obtained by the direct FFT of echo signals following $\pi/2-\tau'-\pi$ pulse sequence, where τ' is time interval between $\pi/2$ and π pulses. Homogeneous line shapes were obtained by the FFT of the decay curves of echo heights as functions of τ'. We applied the magnetic field in the direction of the "magic angle" for the dipolar coupling between ^{13}C pairs to obtain a simple echo decay.

Results are shown in Fig. 8. The inhomogeneous line shape has two sharp peaks at room temperature. This separation comes from the difference in the Knight shift ΔK given above. With decreasing temperature, the inhomogeneous width is gradually broadened. Below 20 K, an asymmetric tail appears but the width of the central line becomes slightly narrowed. This behavior is consistent with the results

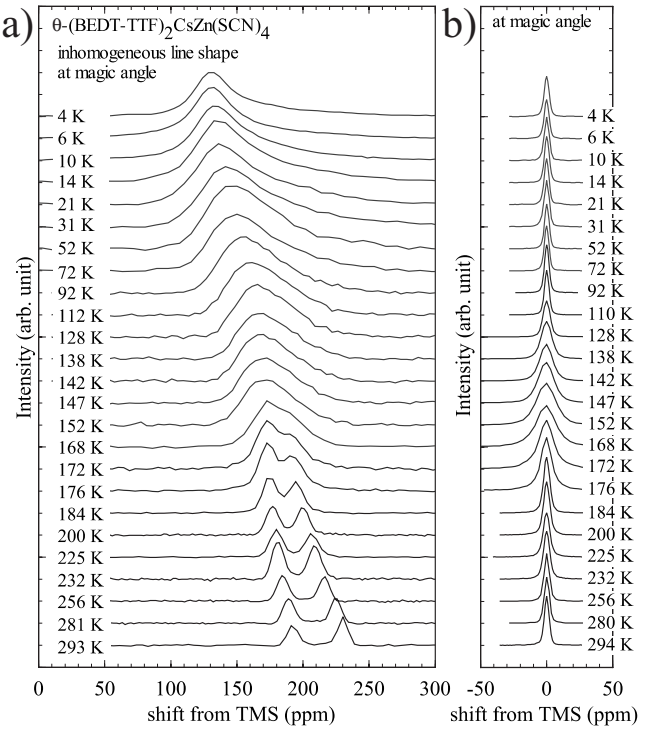

FIG. 8. Temperature dependence of (a) inhomogeneous and (b) homogeneous line shapes of ^{13}C-NMR. The external field was precisely tuned in the *ab* plane to give a magic angle for nuclear dipolar coupling between ^{13}C nuclei.

in Fig. 1. On the other hand, homogeneous line shape exhibits a peculiar feature: At room temperature, a single sharp peak is observed. The linewidth (homogeneous width) becomes broadened as temperature decreases, showing a maximum around 150 K, and then narrowed again. This is quite similar to that observed in the RbZn salt above T_{MI}, so that we apply the same analysis as before.

The large difference between the homogeneous and inhomogeneous linewidths indicates that the large broadening at low temperatures is of inhomogeneous nature. We believe that this is caused by charge disproportionation among the molecular sites on the basis of the above analysis. However, when inhomogeneous fields start to fluctuate in time, the characteristic frequency of the fluctuations $1/\tau_c$ should contribute to reduce the lifetime of the Zeeman levels. As inhomogeneous fields fluctuate more rapidly with increasing temperature, T_2^{-1} also increases. A peak should appear at a temperature where the characteristic frequency becomes comparable to the inhomogeneous width itself (in a frequency scale), since at higher temperatures, the inhomogeneous field should be averaged in time by a well-known motional narrowing process. The peak behavior of the homogeneous width is a clear evidence of dynamic properties of the inhomogeneous fields confirmed above.

Here, $1/T_2$ is defined as the full width at half intensity of homogeneous line shape and plotted in Fig. 9 in a logarithmic scale against the inverse of temperature, in comparison to the results in the RbZn salt. Open circles and closed squares indicate the results of the CsZn salt and the RbZn salt, respectively.

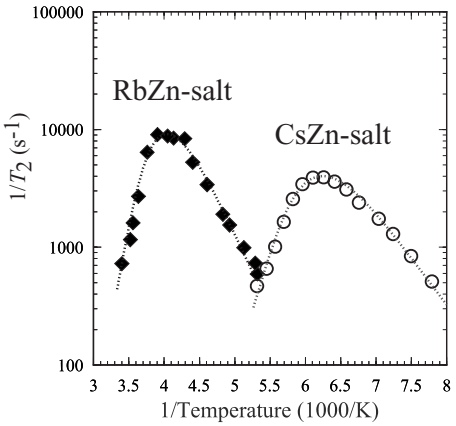

FIG. 9. T_2^{-1} in semilogarithmic scale against the inverse of the temperature. Open circles indicate that of the CsZn salt and diamonds that of the RbZn salt.

To analyze the temperature dependence of $1/T_2$, we applied the same procedure as in the previous work.[18] We assumed that $1/T_2$ is given by the Fourier transformation of an expanded exponential correlation function $\Phi(t)$,

$$\frac{1}{T_2} = \int_{-\infty}^{\infty} \Phi(t)\cos(\sqrt{\langle \Delta\omega^2 \rangle} t)dt,$$

$$\Phi(t) = \langle \Delta\omega^2 \rangle \exp(-(|t|/\tau_c)^{\beta}).$$

Here, τ_c is the correlation time, $\tau_c = \tau_\infty \exp(\Delta/k_B T)$, with a gap energy Δ, the second moment for the inhomogeneous width $\langle \Delta\omega^2 \rangle$, and a parameter β. Dashed lines in Fig. 9 are the fitting curves obtained with the parameters listed in Table I.

Typical correlation times are estimated; τ_c are 2.8×10^{-11}, 1.4×10^{-7}, and 3.3 s at 300, 200, and 120 K, respectively, in the CsZn salt. On the other hand, it is 5.0×10^{-2} s at 200 K in the RbZn salt. We recognized that charge on BEDT-TTF molecule in the CsZn salt can move more easily to another site than that in the RbZn salt.

The parameter $\sqrt{\langle \Delta\omega^2 \rangle}$ is the one characterizing the amplitude of the fluctuating local fields, so that it should be compared with the inhomogeneous width at low temperatures. While the amplitude may be temperature dependent, we neglected it in the above analysis, in comparison to the rapid temperature dependence of τ_c. In the temperature region where the homogeneous width shows a peak, the second moment of the inhomogeneous spectrum is ~ 290 ppm^2, corresponding to $\sqrt{\langle \Delta\omega^2 \rangle}/2\pi \sim 1.5$ kHz, which agrees well to the value describing the homogeneous width. If one compares the second moment with the Knight shift at the center of mass ~ 43 ppm at this temperature, the charge disproportionation is estimated as 0.50 ± 0.20 (standard deviation).

TABLE I. Fitting parameters of temperature dependence of $1/T_2$ on both salts.

	CsZn salt	RbZn salt
β	0.4	0.4
Δ/k_B	5100 K	7600 K
$\sqrt{\langle \Delta\omega^2 \rangle}/2\pi$	1.4 kHz	3.3 kHz

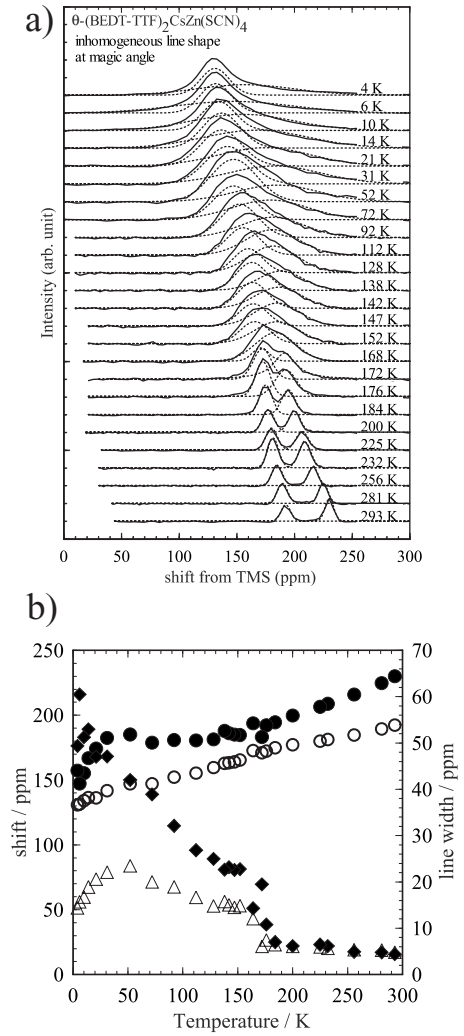

FIG. 10. (a) Inhomogeneous line shape of ^{13}C-NMR shown in Fig. 8(a) was decomposed into two Gaussians with equal intensity. (b) Central shift and linewidth for the two Gaussians are plotted against temperature.

E. Decomposition of inhomogeneous line shape at magic angle

We have tried to decompose the observed inhomogeneous spectra into two Gaussians, as shown in Fig. 10(a). It was successful in the whole temperature range examined except at 4.2 K, and the central shift and the width (square root of the second moment) obtained from the least-squares fittings are plotted in Fig. 10(b). Relative intensity of each Gaussian was always found in the range of 0.5 ± 0.1.

The two peaks observed above 180 K are explained as due to the shift asymmetry ΔK between the double-bonded carbon sites, as mentioned above. The width is almost independent of temperature and agrees well with the homogeneous width. The separation of the peaks gradually decreases

TABLE II. Mean value (standard deviation) of charge distribution for charge-rich and charge-poor site.

T (K)	Charge rich	Charge poor
110	+0.68 (0.26)	+0.31 (0.15)
90	+0.73 (0.40)	+0.26 (0.22)
50	+0.80 (0.63)	+0.20 (0.34)

with decreasing temperature. It is well scaled to static susceptibility. Remarkable broadening below 180 K is caused by the enhancement of the homogeneous width.

The inhomogeneous spectrum is further broadened as temperature decreases below 140 K. In the region between 140 and 50 K, the spectrum can also be decomposed into two Gaussians with equal intensity. These corresponds to the peak and the tail component observed in the analysis of the angular dependence of the spectrum at 101 K (Sec. III B). It should be noted first that the separation of the central shift increases with decreasing temperature, while the center of gravity of the spectrum and thus magnetic susceptibility keep decreasing. Now, the splitting due to ΔK becomes too small to explain the observed separation. Second, the width becomes too large to explain with symmetric charge disproportionation around +0.5. We propose that the two components come from charge-rich and charge-poor sites caused by some short-range charge ordering, as mentioned previously in Sec. III B.

In this temperature region, the system behaves still metallic and there is no anomaly in static susceptibility. Therefore, there is no reason to assume the appearance of local magnetic moments or completely different magnetic behavior between the charge-rich and charge-poor sites. We simply assumed that the local susceptibility is proportional to the effective charge at each molecular site and that the central shift of the whole spectrum from the chemical shift ~135 ppm corresponds to the averaged molecular charge of +0.5. We thus estimated the mean value and standard deviation of charge distribution for each component. Results are shown in Table II.

The charge disproportionation seems further develop with decreasing temperature. The distribution width is again too large to explain with charge disproportionation. This suggests the existence of some unknown mechanism of line broadening, as discussed for the charge-rich sites in the RbZn salt below T_{MI}.

Below 30 K, a qualitative change in spectrum appears; the asymmetry is further enhanced with a longer tail and a sharper peak. The half width of the spectrum starts to decrease, while the second moment keeps increasing as temperature decreases. We are not sure that the decomposition applied at higher temperatures is still valid in this region because of the ambiguity due to the long tail contribution. However, the results of tentative decomposition in Fig. 10(b) suggest that the narrower component moves almost linearly toward the zero Knight shift position and the width starts to decrease at low temperatures. In addition, the central shift of the broader component also decreases below 30 K, while it seems to tend to a finite value. It is clear that the narrower component is the one assigned as the peak whose anisotropy was discussed in Sec. III C and the broader one as the tail. We have already pointed out that the narrow peak cannot be assigned to charge-poor sites but the effective charge is expected as +0.5 with relatively small distribution (± 0.16). This strongly suggests that a qualitative change in the electronic state takes place around 30 K. We will discuss this issue in the next section in comparison to the other experimental results.

F. Relation to the other experimental results and theories

From the experimental results described above, it is clear that the electronic properties in the CsZn salt can be divided into three which correspond to three different temperature regions: (I) the high temperature region from room temperature down to 140 K, (II) the intermediate region between 140 and 50 K, and (III) the low temperature region below 30 K. At high temperatures in region (I), we have observed the development of large charge disproportionation and the slowing down of charge fluctuations with decreasing temperature. It is quite similar to that observed in the isostructural compound, the RbZn salt.[18] The charge disproportionation in this region is estimated as 0.50 ± 0.20 (standard deviation) and is motionally narrowed at high temperatures.

In the intermediate region [region (II)], the charge fluctuation becomes extremely slow and almost static in the time scale of ^{13}C-NMR. The anisotropic spectrum suggests that a short-range charge ordering of the charge-poor and charge-rich sites seems to develop in this region. This is in good agreement with the results of x-ray measurements: Watanabe and co-workers reported that two different types of short-range lattice modulations with $q_1=(2/3,k,1/3)$ and $q_2=(0,k,1/2)$ grow below 120 K.[30,31] The q_2 modulation corresponds to the one for the horizontal stripes confirmed in the RbZn salt. The q_1 modulation with threefold periodicity was first suggested by Mori,[44] who examined the stability of charge distribution, considering the anisotropy of intermolecular Coulomb energy estimated by the extend Hückel approximation. Kaneko and Ogata investigated a 1/4-filled extended Hubbard model on an anisotropic triangular lattice and found that a metallic charge ordering with threefold periodicity is realized when nearest neighbor Coulomb interaction V is nearly isotropic.[45]

It should be noted that these different short-range orderings coexist and probably compete with each other, which should prohibit the formation of any long-range ordering down to low temperatures. As for the stability of different types of charge orderings, there are many theoretical considerations.[2,3] From a study of a triangular model with mean field approximation by Hotta, the stabilization of charge ordering is mapped in schematic phase diagram with transfer integral where the phase boundary is located between the RbZn and the CsZn salts.[46] It was pointed out that the competition between different charge ordering patterns can lead to a quantum melting of charge ordering by calculations including quantum fluctuation by Merino *et al.*[47] and the variational Monte Carlo method.[48] Various metallic states

with different charge modulations and large charge fluctuations are expected theoretically.[47] It is quite suggestive that this salt in region (II) behaves metallically in spite of such large charge disproportionation.

The temperature region [region (III)] roughly corresponds to the one where the nonmetallic conduction appears.[25,28] The present ^{13}C-NMR spectrum suggests the coexistence of spin-singlet molecular sites without large charge ordering and paramagnetic sites with finite magnetic susceptibility. This means that charge distribution should have been rearranged at low temperatures.

Possibility of a phase transition at 20 K was pointed out by EPR measurements by Nakamura *et al.*,[29] who made a precise analysis of the principal values of g tensor and found that the principal axes gradually rotate with decreasing temperature and at 15 K, suddenly turn back to the initial direction at high temperatures. The authors claimed the existence of charge disproportionation at high temperatures and of the charge redistribution below 20 K. These results are consistent with the present results of ^{13}C-NMR measurements.

Rearrangement of charge accompanying spin-singlet formation has been reported in a different system: Fujiyama and Nakamura observed a splitting of ^{13}C-NMR spectrum due to charge ordering in a one-dimensional organic conductor, $(TMTTF)_2AsF_6$, which merges again at the spin-Peierls transition, implying a redistribution of charge densities.[49] A possible spin-singlet ground state without charge ordering is the $4k_F$ bond-order wave (BOW) state, which was theoretically predicted in one-dimensional conductors by Clay *et al.*[50] It may be one of the possible explanations of the present results, while we do not have any direct evidence for this model to be applicable in our system. We only claim that the spin-singlet state in the CsZn salt is quite different from the one observed in a charge-ordered state in the RbZn salt. It should be noted that the system is largely inhomogeneous since almost half of the molecular sites are paramagnetic with finite susceptibility. Kanoda *et al.* carried out ^{13}C-NMR measurements in the present salt and claimed that the system is in a charge-glass state.[51] On the other hand, Raman and infrared spectroscopies show no indication of large-amplitude charge ordering.[52]

Recently, curious conducting behaviors at low temperatures were reported in this system. Sawano *et al.* found a giant nonlinear resistance and thyristor I-V characteristics.[34] Takahide *et al.* observed a power-law behavior in the I-V characteristics in θ-$(BEDT\text{-}TT)_2MZn(SCN)_4[M=Rb,Cs]$ and claimed that it is caused by the unbinding of thermally excited electron-hole pairs from the charge-ordered ground state.[53]

IV. CONCLUSION

We have investigated the electronic states in θ-$(BEDT\text{-}TTF)_2CsZn(SCN)_4$ by analyzing ^{13}C-NMR spectra in a selectively ^{13}C-enriched single crystal samples. We have found that it can be divided into three which correspond to three different temperature regions, (I) the high temperature region from room temperature down to ~140 K, (II) the intermediate region between 140 and 50 K, and (III) the low temperature region below ~30 K. In region (I), remarkable charge disproportionation with extremely slow fluctuations was observed, just as in the metallic state of the RbZn salt. Correlation time of the charge fluctuation in the CsZn salt is shorter than that in the RbZn salt, which implies that charges are hopping around more frequently.

In region (II), the charge disproportionation becomes almost static, forming a short-range charge ordering. The absence of long-range ordering should be due to the competition between the different types of charge ordering detected by x-ray measurements. This situation is well understood if we consider that the CsZn salt is located on the phase boundary derived theoretically. In the insulating region [region III], no long-range charge ordering is stabilized, contrary to the case of the RbZn salt. Instead, about half of the molecular sites become nonmagnetic, while the other half carry finite magnetic moment. The charge disproportionation becomes very much reduced at least at the nonmagnetic molecular sites, implying that charge rearrangement should have occurred. It is consistent with the results of Raman spectroscopy. Spin-singlet states with uniform charge are reminiscent of the $4k_F$ BOW ground state predicted for one-dimensional systems.

The electronic state in the CsZn salt was much more complicated than that in the RbZn salt because of the competition between different types of charge ordering. The lack of long-range ordering is the origin of unique electromagnetic properties, such as extremely large dielectric anomalies, nonlinear transport properties, the "thyristor" effect, and so on. The present ^{13}C-NMR measurements have clarified the nature of the charge inhomogeneity from microscopic point of view.

ACKNOWLEDGMENTS

The authors greatly appreciate fruitful discussions with K. Kanoda, K. Miyagawa, Y. Takano, Y. Nogami, M. Watanabe, H. Seo, C. Hotta, Y. Suzumura, and H. Fukuyama. Thanks are also due to M. Yazawa for informing the authors of her unpublished data along the c axis. The authors are grateful for the financial support from Grant-in-Aid for Scientific Research on Priority Areas of Molecular Conductors (No. 15073221) from the Ministry of Education, Culture, Sports, Science, and Technology, Japan.

*Present address: National Institute of Advanced Industrial Science and Technology, 1-1-1, Higashi, Tsukuba, Ibaraki 305-8573, Japan.

[1] T. Takahashi, Y. Nogami, and K. Yakushi, J. Phys. Soc. Jpn. **75**, 051008 (2006).

[2] H. Seo, C. Hotta, and H. Fukuyama, Chem. Rev. (Washington, D.C.) **104**, 5005 (2004).

[3] H. Seo, J. Merino, H. Yoshioka, and M. Ogata, J. Phys. Soc. Jpn. **75**, 051009 (2006).

[4] K. Hiraki and K. Kanoda, Phys. Rev. Lett. **80**, 4737 (1998).

[5] T. Nakamura, T. Nobutoki, Y. Kobayashi, T. Takahashi, and G. Saito, Synth. Met. **70**, 1293 (1995).

[6] H. Seo and H. Fukuyama, J. Phys. Soc. Jpn. **66**, 1249 (1997).

[7] D. S. Chow, F. Zamborszky, B. Alavi, D. J. Tantillo, A. Baur, C. A. Merlic, and S. E. Brown, Phys. Rev. Lett. **85**, 1698 (2000).

[8] F. Zamborszky, W. Yu, W. Raas, S. E. Brown, B. Alavi, C. A. Merlic, and A. Baur, Phys. Rev. B **66**, 081103(R) (2002).

[9] F. Nad, P. Monceau, C. Carcel, and J. M. Fabre, Phys. Rev. B **62**, 1753 (2000).

[10] P. Monceau, F. Y. Nad, and S. Brazovskii, Phys. Rev. Lett. **86**, 4080 (2001).

[11] K. Miyagawa, A. Kawamoto, and K. Kanoda, Phys. Rev. B **62**, R7679 (2000).

[12] R. Chiba, H. Yamamoto, K. Hiraki, T. Takahashi, and T. Nakamura, J. Phys. Chem. Solids **62**, 393 (2001).

[13] Y. Takano, H. M. Yamamoto, K. Hiraki, T. Nakamura, and T. Takahashi, J. Phys. Chem. Solids **62**, 389 (2001).

[14] Y. Takano, K. Hiraki, H. M. Yamamoto, T. Nakamura, and T. Takahashi, Synth. Met. **120**, 1081 (2001).

[15] H. Kino and H. Fukuyama, J. Phys. Soc. Jpn. **65**, 2158 (1996).

[16] H. Seo, J. Phys. Soc. Jpn. **69**, 805 (2000).

[17] T. Itou, K. Kanoda, K. Murata, T. Matsumoto, K. Hiraki, and T. Takahashi, Phys. Rev. Lett. **93**, 216408 (2004).

[18] R. Chiba, K. Hiraki, T. Takahashi, H. M. Yamamoto, and T. Nakamura, Phys. Rev. Lett. **93**, 216405 (2004).

[19] S. Moroto, K. Hiraki, Y. Takano, Y. Kubo, T. Takahashi, H. M. Yamamoto, and T. Nakamura, J. Phys. IV **114**, 399 (2004).

[20] A. F. Bangura, A. I. Coldea, J. Singleton, A. Ardavan, A. Akutsu-Sato, H. Akutsu, S. S. Turner, P. Day, T. Yamamoto, and K. Yakushi, Phys. Rev. B **72**, 014543 (2005).

[21] P. Littlewood, Nature (London) **399**, 529 (1999).

[22] M. Watanabe, Y. Noda, Y. Nogami, and H. Mori, J. Phys. Soc. Jpn. **73**, 116 (2004).

[23] K. Yamamoto, K. Yakushi, K. Miyagawa, K. Kanoda, and A. Kawamoto, Phys. Rev. B **65**, 085110 (2002).

[24] H. Tajima, S. Kyoden, H. Mori, and S. Tanaka, Phys. Rev. B **62**, 9378 (2000).

[25] H. Mori, S. Tanaka, and T. Mori, Phys. Rev. B **57**, 12023 (1998).

[26] M. Watanabe, Y. Noda, Y. Nogami, and H. Mori, J. Phys. Soc. Jpn. **74**, 2011 (2005).

[27] Kenji Suzuki, Kaoru Yamamoto, and Kyuya Yakushi, Phys. Rev. B **69**, 085114 (2004).

[28] H. Mori, S. Tanaka, T. Mori, A. Kobayashi, and H. Kobayashi, Bull. Chem. Soc. Jpn. **71**, 797 (1998).

[29] T. Nakamura, W. Minagawa, R. Kinami, and T. Takahashi, J. Phys. Soc. Jpn. **69**, 504 (2000).

[30] Y. Nogami, J. P. Pouget, M. Watanabe, K. Oshima, H. Mori, S. Tanaka, and T. Mori, Synth. Met. **103**, 1911 (1999).

[31] M. Watanabe, Y. Nogami, K. Oshima, H. Mori, and S. Tanaka, J. Phys. Soc. Jpn. **68**, 2654 (1999).

[32] H. Mori, T. Okano, S. Tanaka, M. Tamura, Y. Nishio, K. Kajita, and T. Mori, J. Phys. Soc. Jpn. **69**, 1751 (1999).

[33] K. Inagaki, I. Terasaki, H. Mori, and T. Mori, J. Phys. Soc. Jpn. **73**, 3364 (2004).

[34] F. Sawano, I. Terasaki, H. Mori, T. Mori, M. Watanabe, N. Ikeda, Y. Nogami, and Y. Noda, Nature (London) **437**, 04087 (2005).

[35] S. Fujiyama, M. Takigawa, and S. Horii, Phys. Rev. Lett. **90**, 147004 (2003).

[36] R. Chiba, K. Hiraki, T. Takahashi, H. M. Yamamoto, and T. Nakamura, Synth. Met. **133-134**, 305 (2003).

[37] R. Chiba, K. Hiraki, T. Takahashi, H. M. Yamamoto, and T. Nakamura, Synth. Met. **135-136**, 595 (2003).

[38] T. Takahashi, K. Hiraki, S. Moroto, N. Tajima, Y. Takano, Y. Kubo, H. Satsukawa, R. Chiba, H. M. Yamamoto, R. Kato, and T. Naito, J. Phys. IV **131**, 3 (2005).

[39] M. Yazawa (private communication).

[40] H. Mayaffre, P. Wzietek, D. Jérome, C. Lenoir, and P. Batail, Phys. Rev. Lett. **75**, 4122 (1995).

[41] A. Kawamoto, K. Miyagawa, Y. Nakazawa, and K. Kanoda, Phys. Rev. B **52**, 15522 (1995).

[42] K. Miyagawa, A. Kawamoto, and K. Kanoda, Phys. Rev. B **56**, R8487 (1997).

[43] H. Mori, S. Tanaka, T. Mori, and Y. Maruyama, Bull. Chem. Soc. Jpn. **68**, 1136 (1995).

[44] T. Mori, Bull. Chem. Soc. Jpn. **73**, 2243 (2000).

[45] M. Kaneko and M. Ogata, J. Phys. Soc. Jpn. **75**, 014710 (2006).

[46] C. Hotta, J. Phys. Soc. Jpn. **72**, 840 (2003).

[47] J. Merino, H. Seo, and M. Ogata, Phys. Rev. B **71**, 125111 (2005).

[48] H. Watanabe and M. Ogata, J. Phys. Soc. Jpn. **75**, 063702 (2006).

[49] S. Fujiyama and T. Nakamura, J. Phys. Soc. Jpn. **75**, 014705 (2006).

[50] R. T. Clay, S. Mazumdar, and D. K. Campbell, Phys. Rev. B **67**, 115121 (2003).

[51] K. Kanoda, K. Ohnou, M. Kodama, K. Miyagawsa, T. Itou, and K. Hiraki, J. Phys. IV **131**, 21 (2005).

[52] K. Suzuki, K. Yamamoto, K. Yakushi, and A. Kawamoto, J. Phys. Soc. Jpn. **74**, 2631 (2005).

[53] Y. Takahide, T. Konoike, K. Enomoto, M. Nishimura, T. Terashima, S. Uji, and H. M. Yamamoto, Phys. Rev. Lett. **96**, 136602 (2006).